Check for updates

Andrology

WILEY

ANDROLOGY

ORIGINAL ARTICLE

Dynamic Landscape of H3K4me3 and H3K27me3 Modification During Postnatal Leydig Cell Fate Determination

Jiandong Sun[1,2] | Xiuli Lian[1,2] | Shanshan Luo[1] | Zihang Lin[1] | Lvjing Luo[1] | Mei Zheng[1] | Dini Zhang[1] | Zeyu Lin[1] | Xuanyi Wang[1] | Shie Wang[1,2]

[1]Key Laboratory of Stem Cell Engineering and Regenerative Medicine of Fujian Province University, Fujian Medical University, Fuzhou, P. R. China | [2]Department of Histology and Embryology, School of Basic Medical Sciences, Fujian Medical University, Fuzhou, P. R. China

Correspondence: Shie Wang (shiewang@fjmu.edu.cn)

Received: 4 July 2025 | **Revised:** 10 November 2025 | **Accepted:** 9 December 2025

Keywords: bivalent | epigenetic reprogramming | H3K4me3 | H3K27me3 | Leydig cells | lineage commitment

ABSTRACT

Background: Histone methylation plays a crucial role in regulating chromatin architecture and gene expression during spermatogenesis. H3K4me3 is enriched at the transcription start sites of active genes, whereas H3K27me3 is deposited on chromatin to confer transcriptional repression. However, the dynamics of H3K4me3 and H3K27me3 modifications in the differentiation of postnatal Leydig cells remain poorly characterized.

Objectives: The purpose of this study was to elucidate the dynamics of H3K4me3 and H3K27me3 modifications in the differentiation of postnatal Leydig cells.

Methods: Through an integrated analysis of single-cell RNA-seq (scRNA-seq), cleavage under targets and tagmentation sequencing (CUT&Tag-seq), bulk RNA-seq, and immunohistochemistry across different developmental stages of mouse Leydig cells, we mapped the stage-specific landscapes of H3K4me3 and H3K27me3.

Results: Our results demonstrate that during progenitor to immature Leydig cell differentiation, H3K4me3 levels exhibited a diphasic fluctuation pattern (first decreasing and then increasing), contrasting with the progressive accumulation of H3K27me3. In progenitor Leydig cells, the resolution of bivalent chromatin domains (accounting for 24.5% of promoters) helps balance cell proliferation and differentiation. Strikingly, steroidogenic genes such as *Star*, *Cyp17a1*, and *Hsd17b3* are exclusively regulated by H3K4me3 and lack H3K27me3 marking. In terminally differentiated adult Leydig cells, H3K4me3 sustains the steroidogenic capacity by activating transcription factors (such as *Gata6*, *Cebpb*, *Nr1d1*) and maturation markers (including *Hsd17b3*, *Insl3*, *Sult1e1*), while H3K27me3 permanently silences proliferation-related networks (such as *Ccna2*, *Mki67*, *Ccnd1*) to eliminate the self-renewal potential of these cells.

Discussion and Conclusion: Our work identifies an H3K4me3/H3K27me3-transcription factors (TFs)-target gene axis as a central regulatory mechanism governing postnatal Leydig cell differentiation. This discovery clarifies how this axis endows Leydig cells with steroidogenic potential while suppressing stemness properties.

Jiandong Sun, Xiuli Lian, and Shanshan Luo contributed equally to this work.

© 2025 American Society of Andrology and European Academy of Andrology.

1 | Introduction

Leydig cells serve as the principal source of testosterone in males, undergoing a well-defined developmental progression postnatally through four distinct stages: stem Leydig cells (SLCs), progenitor Leydig cells (PLCs), immature Leydig cells (ILCs), and adult Leydig cells (ALCs) [1]. In the murine model, PLCs emerge by postnatal day 14 (PND14) and are characterized by the expression of marker genes, including *Arx*, *Nr2f2*, and *Pdgfra*, as well as steroidogenic enzymes like *Cyp11a1* and *Hsd3b1* [2]. Subsequently, PLCs transition into lipid droplet-laden ILCs by PND28, and then further maturation into ALCs by PND56. This maturation process is marked by the progressive upregulation of *Hsd17b3*, conferring upon ALCs the capacity for autonomous testosterone synthesis [3, 4].

The lineage commitment of postnatal Leydig cells is precisely orchestrated through the coordinated actions of multiple signaling pathways and transcriptional regulators. For instance, Sertoli cell-derived Desert hedgehog (DHH) interacts with the Patched (PTCH) receptor on PLCs, relieving PTCH-mediated suppression of Smoothened (SMO). This permits SMO to activate GLIs-mediated transcription, thereby initiating Leydig cell differentiation [5, 6]. Conversely, Notch signaling functions as a potent negative regulator of this process. Pharmacological inhibition of Notch signaling significantly promotes steroidogenic lineage commitment from SLCs to ALCs in rat seminiferous tubule cultures [7]. Activation of the Smad pathway also inhibits PLC differentiation [8]. Among transcriptional regulators, steroidogenic factor-1 (SF-1) is indispensable for Leydig cell fate determination [9]. Notably, SF-1 overexpression has been demonstrated to direct the differentiation of embryonic stem cells/pluripotent stem cells into Leydig-like cells [10, 11].

Current research on histone methylation modifications during ALCs differentiation remains remarkably limited, and few systematic comparative analyses have been reported to date. Modifications of Histone 3 at lysine residues 4 (H3K4) and 27 (H3K27) represent pivotal epigenetic regulators that govern gene expression programs and cell fate decisions. The activating mark H3K4me3 facilitates transcriptional activation by recruiting chromatin remodelers and histone acetyltransferase complexes [12–14]. In contrast, the repressive H3K27me3 modification establishes transcriptional silencing by mediating chromatin condensation. In the present study, we comprehensively characterize the dynamic patterns of H3K4me3 and H3K27me3 during ALCs development, establishing their functional significance in driving the transcriptional reprogramming that orchestrates progenitor cell commitment and terminal maturation.

2 | Methods

2.1 | Leydig Cells Acquisition

ICR male mice were purchased from Fujian Medical University. This study was approved by the local ethics committee of Fujian Medical University (Code of Ethics: LLSLBH-20210930–002). Leydig cells at various developmental stages were isolated from ICR male mice. PLCs were obtained from 2-week-old mice, ILCs from 4/5-week-old mice, and ALCs from 8-week-old mice. After sacrificing the mice, the testes were immediately collected, enzymatically digested with collagenase, filtered through a nylon mesh, and purified by Percoll gradient centrifugation to obtain Leydig cell fractions.

2.2 | Leydig Cell Identification

Progenitor Leydig cells were fixed with paraformaldehyde, permeabilized with Triton X-100, blocked with BSA, and then incubated with anti-NR2F2 antibody (Abconal; Cat#A24647) overnight. On the following day, after incubation with the secondary antibody and DAPI, the NR2F2-positive cells were visualized using a fluorescence microscope. Detailed information regarding the antibodies used is provided in Table S1.

Immature Leydig cells and adult Leydig cells were identified by HSD3B1 staining according to our established protocol. In brief, Solution A (10 mg of β-NAD in 9.5 mL of PBS) was mixed with Solution B (0.6 mg of DHEA + 1 mg of NBT in 0.6 mL of DMSO) at a ratio of 188:12. After a 2 h incubation, positive cells were quantified under a light microscope.

Adult Leydig cells were additionally confirmed by HSD17B3 (Proteintech; Cat# 13415-1-AP) immunofluorescence staining.

2.3 | Immunohistochemistry

Testes removed from mice were fixed with 4% paraformaldehyde, dehydrated in a gradient of 20%–30% sucrose solution, embedded in optimal cutting temperature compound, and then sectioned at a thickness of 10 μm. The sections were treated with 3% H_2O_2, blocked with 5% BSA, and then incubated with H3K4me3 and H3K27me3 antibodies overnight. Next, the samples were processed using an immunohistochemistry detection kit (Zsbio, China; Cat#PV-9001) and visualized with diaminobenzidine (Zsbio, China; Cat#ZLI-9018). Detailed information regarding the antibodies used is provided in Table S1.

2.4 | Single-Cell RNA Sequencing

Testicular samples from C57BL/6 mice were collected at various developmental time points to profile normal testicular development. The data are publicly available in the GEO repository under accession number GSE211115. Furthermore, we used the Male Health Atlas (MHA) platform (www. malehealthatlas.cn), an interactive online resource, to visualize and analyze the single-cell RNA sequencing data.

2.5 | CUT&Tag Sequencing

In accordance with the manufacturer's protocol, approximately 10^5 Leydig cells per group were incubated with ConA beads. Subsequently, the complexes were incubated with either anti-H3K4me3 (Cell Signaling Technology, Cat#9751), anti-H3K27me3 (Cell Signaling Technology; Cat#9733), or normal IgG as a control overnight, followed by hatching secondary antibodies and pG-Tn5 transposase for tagmentation. The resulting DNA

20472927, 0, Downloaded from https://onlinelibrary.wiley.com/doi/10.1111/andr.70165 by Sun jiandong - Fujian Medical University , Wiley Online Library on [22/12/2025]. See the Terms and Conditions (https://onlinelibrary.wiley.com/terms-and-conditions) on Wiley Online Library for rules of use; OA articles are governed by the applicable Creative Commons License

fragments were purified, ligated with an adapter, and processed for library construction. Finally, they were sent to Wuhan Igenebook Biotechnology Co., Ltd. for sequencing (see "Supplemental material"). CUT&Tag sequencing data were deposited in the National Genomics Data Center (NGDC) database with accession number CRA032246.

2.6 | RT-qPCR

Total RNA was extracted using the E.Z.N.A. Total RNA Kit I (Vazyme, China), and cDNA was synthesized from the RNA following the instructions of the PrimeScript RT reagent kit (Takara, Japan). Amplification was then performed using ChamQ SYBR qPCR Master Mix (Vazyme) on a real-time PCR instrument. The primer sequences used in this study are shown in Table S2.

2.7 | RNA Sequencing

Leydig cells isolated from 4- and 8-week-old mice were harvested and underwent RNA extraction with a total RNA extraction kit. The RNA samples were then submitted to Majorbio Technology Co., Ltd. for library construction and sequencing (see "Supplemental material"). RNA sequencing data were deposited in the National Genomics Data Center (NGDC) database with accession number CRA032246.

3 | Results

3.1 | Stage-Specific H3K4me3 and H3K27me3 Dynamics in Postnatal Leydig Cells

Histone modifications are dynamically regulated by specialized enzymatic machinery. Histone lysine methyltransferases (KMTs) serve as "writers" to deposit methyl marks, while lysine demethylases (KDMs) act as "erasers" to remove these modifications.

H3K4me3 is a canonical epigenetic marker of active transcription. The KDM5 subfamily (including KDM5A-D) demethylates tri-methylated H3K4, whereas the COMPASS-like complex (containing KMT2A-D) deposits this activation mark [15] (Figure 1A). Through single-cell RNA sequencing of mouse testis tissues across seven developmental stages (GSE211115), we found a significant transient upregulation of the methyltransferase *Kmt2a* and *Kmt2c* at PND14 (Figure 1B–D). Additionally, the expression of demethylases *Kdm5a* and *Kdm5b* decreased at PND35 during the differentiation of progenitor cells into immature Leydig cells (Figure 1D; Figure S1). Immunohistochemistry further demonstrated that H3K4me3 levels decreased from early progenitor Leydig cells (PND14) to late progenitor Leydig cells (PND21) and subsequently increased during the transition to immature Leydig cells (Figure 1E).

H3K27me3 is a fundamental epigenetic mark mediating transcriptional repression. The polycomb repressive complex 2 (PRC2) subunits, EZH1 and EZH2, catalyze the deposition of H3K27me3. Conversely, the Jumonji-domain demethylases, KDM6A, KDM6B, and UTY, remove this mark to alleviate transcriptional repression [15]. Late-progenitor Leydig cells (PND21) demonstrated significant H3K27me3 accumulation, concomitant with upregulation of *Ezh2* expression and downregulation of *Kdm6b* expression (Figure 1D–E; Figures S1–S3). It suggested that H3K27me3 may facilitate the transition from the progenitor to the committed lineage stages by silencing stemness genes.

3.2 | H3K4me3 Enrichment Profiles in the Progenitor Leydig Cells and Immature Leydig Cells

To explore H3K4me3-mediated transcriptional reprogramming during postnatal Leydig cell differentiation, CUT&Tag sequencing was employed to map the profile genome-wide distribution of H3K4me3 in purified progenitor (PND14) and immature (PND35) Leydig cell populations (Figure 2A,B; Figure S2). Approximately 10.87% of promoters exhibited significantly higher H3K4me3 enrichment in progenitor Leydig cells versus immature Leydig cells ($p < 0.01$). A larger proportion (21.83%) showed enhanced occupancy at the immature cells stage, suggesting stage-specific transcriptional priming (Figure 2C,D).

Kyoto Encyclopedia of Genes and Genomes (KEGG) enrichment analysis demonstrated that H3K4me3-enriched genes in PND14 progenitor Leydig cells were predominantly associated with the Hedgehog signaling pathway, the Hippo signaling pathway, and signaling pathways regulating the pluripotency of stem cells (Figure 2E). Gene Ontology (GO) analysis further revealed that H3K4me3-marked genes in progenitor cells were involved in somatic stem cell maintenance, the kit signaling pathway, and cell fate commitment. In contrast, in PND35 immature Leydig cells, H3K4me3 was preferentially associated with testosterone biosynthesis, spermatogenesis-related processes (including flagellated sperm motility and spermatid nucleus elongation), and male gonad development (Figure 2F). RT-qPCR also indicated that the expression of *Star*, *Cyp17a1*, and *Hsd17b3* was decreased following *Kmt2c* knockdown in PND35 immature Leydig cells (Figure S4).

Furthermore, genomic visualization using IGV software revealed distinct H3K4me3 occupancy patterns at critical developmental loci across the progenitor and the immature Leydig cell stages (Figure S5). It was observed that there was a progressive loss of this activation mark at progenitor-specific loci, including core progenitor markers (*Arx*, *Tcf21*, *Pdgfra*) and Desert hedgehog signaling components (*Dhh*, *Gli1/2*, *Smo*). Conversely, steroidogenic genes (*Star*, *Cyp17a1*, *Hsd17b3*) and adult Leydig cell markers (*Insl3*, *Sult1e1*, *Ptgds*) showed stage-dependent acquisition of H3K4me3.

3.3 | H3K27me3 Enrichment Profiles in the Progenitor Leydig Cells and Immature Leydig Cells

H3K27me3 also showed strongly correlated occupancy changes at promoters during the differentiation of Leydig cells (Figure 3A,B). Quantitative analysis revealed stage-specific enrichment profiles: 12.67% of promoters maintained significantly higher H3K27me3 levels in progenitor cells ($p < 0.01$), while a larger proportion (26.07%) showed elevated H3K27me3 deposition in immature Leydig cells (Figure 3C,D). Notably, H3K27me3-enriched genes in PND35 immature Leydig cells were significantly associated

20472927, 0, Downloaded from https://onlinelibrary.wiley.com/doi/10.1111/andr.70165 by Sun jiandong - Fujian Medical University , Wiley Online Library on [22/12/2025]. See the Terms and Conditions (https://onlinelibrary.wiley.com/terms-and-conditions) on Wiley Online Library for rules of use; OA articles are governed by the applicable Creative Commons License

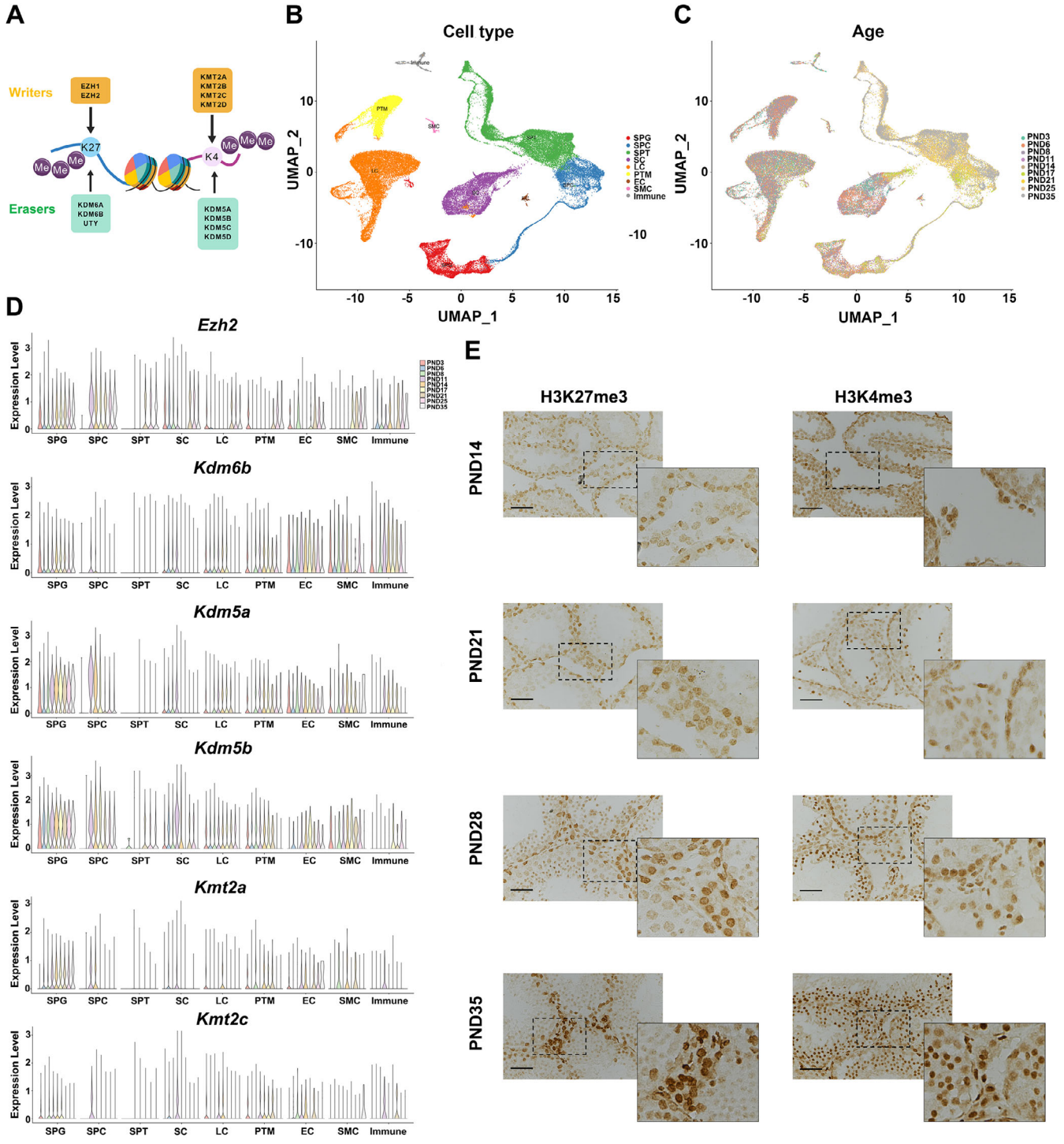

FIGURE 1 | Stage-specific H3K4me3 and H3K27me3 dynamics in postnatal Leydig cells. (A) Schematic depicting methyltransferases (writers) and demethylases (erasers) controlling dimethyl-to-trimethyl conversion at H3K4 and H3K27 residues. (B, C) UMAP visualization of testicular single-cell transcriptomes from PND3-PND35 mice. (D) Expression levels of H3K4me3/H3K27me3-modifying enzymes (writers/erasers) visualized by organ chart across Leydig cell developmental stages. (E) Representative immunohistochemical staining for H3K4me3 and H3K27me3 in progenitor (PND14,21) and immature (PND28,35) Leydig cells. Scale bar, 50 μm. EC: endothelial cells; Immune, immune cell; LC, Leydig cells; PTM: peritubular myoid cells; SC: Sertoli cells; SMC: vascular smooth muscle cells; SPC, spermatocytes; SPG, spermatogonia; SPT, spermatids/sperms.

20472927, 0, Downloaded from https://onlinelibrary.wiley.com/doi/10.1111/andr.70165 by Sun jiandong - Fujian Medical University , Wiley Online Library on [22/12/2025]. See the Terms and Conditions (https://onlinelibrary.wiley.com/terms-and-conditions) on Wiley Online Library for rules of use; OA articles are governed by the applicable Creative Commons License

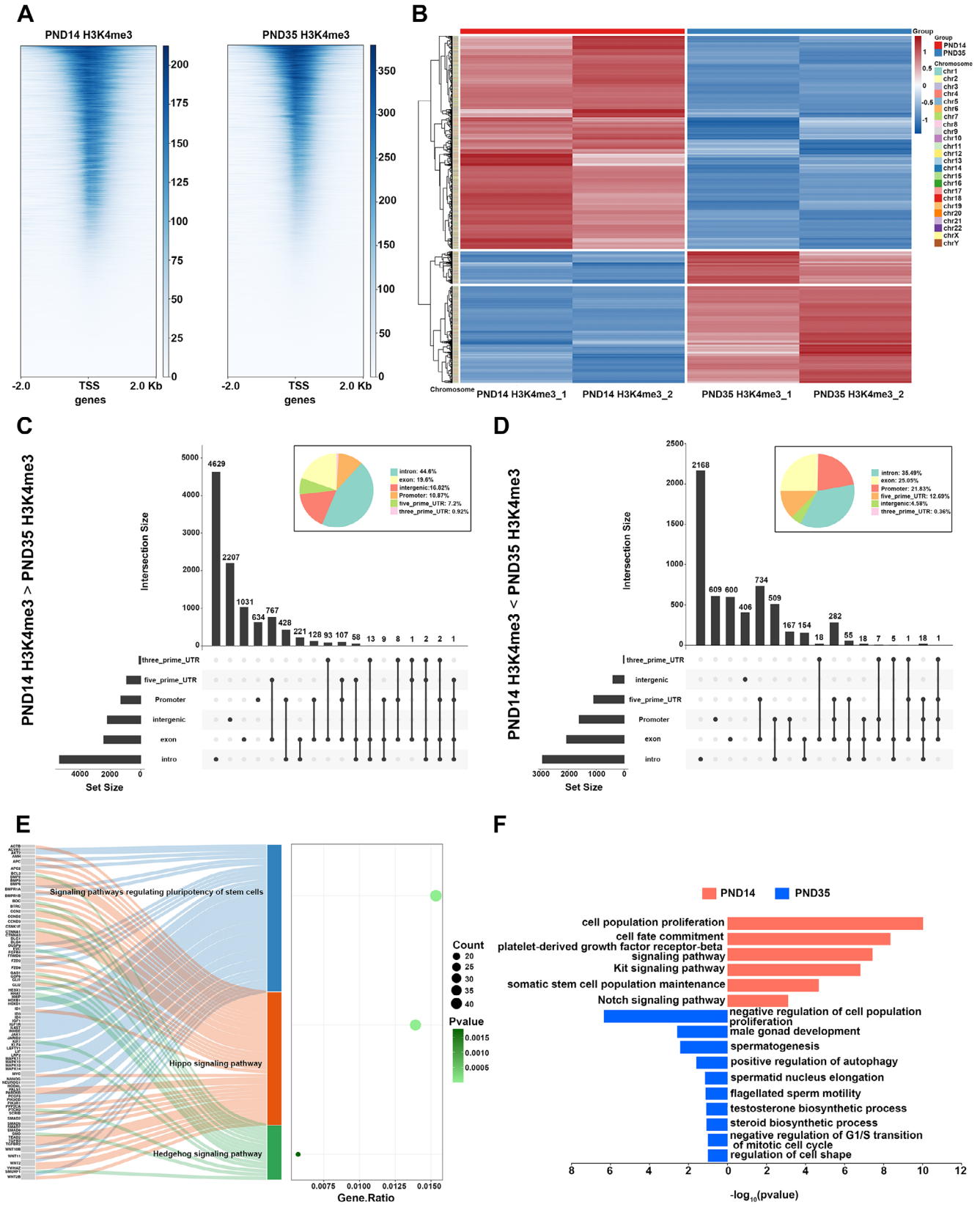

FIGURE 2 | H3K4me3 enrichment profiles in the progenitor Leydig cells and immature Leydig cells. (A) Heatmap of H3K4me3 enrichment at transcription start sites of annotated genes. (B) Differentially enriched H3K4me3 peaks between PND14 and PND35 Leydig cells. (C, D) Upset plots depicting unique sets of H3K4me3-enriched genomic regions in PND14 and PND35 Leydig cells. (E) KEGG pathway enrichment analysis of genes associated with H3K4me3 peaks in PND14 Leydig cells. (F) GO biological process enrichment analysis of genes associated with H3K4me3 peaks in PND14 and PND35 Leydig cells.

20472927, 0, Downloaded from https://onlinelibrary.wiley.com/doi/10.1111/andr.70165 by Sun jiandong - Fujian Medical University , Wiley Online Library on [22/12/2025]. See the Terms and Conditions (https://onlinelibrary.wiley.com/terms-and-conditions) on Wiley Online Library for rules of use; OA articles are governed by the applicable Creative Commons License

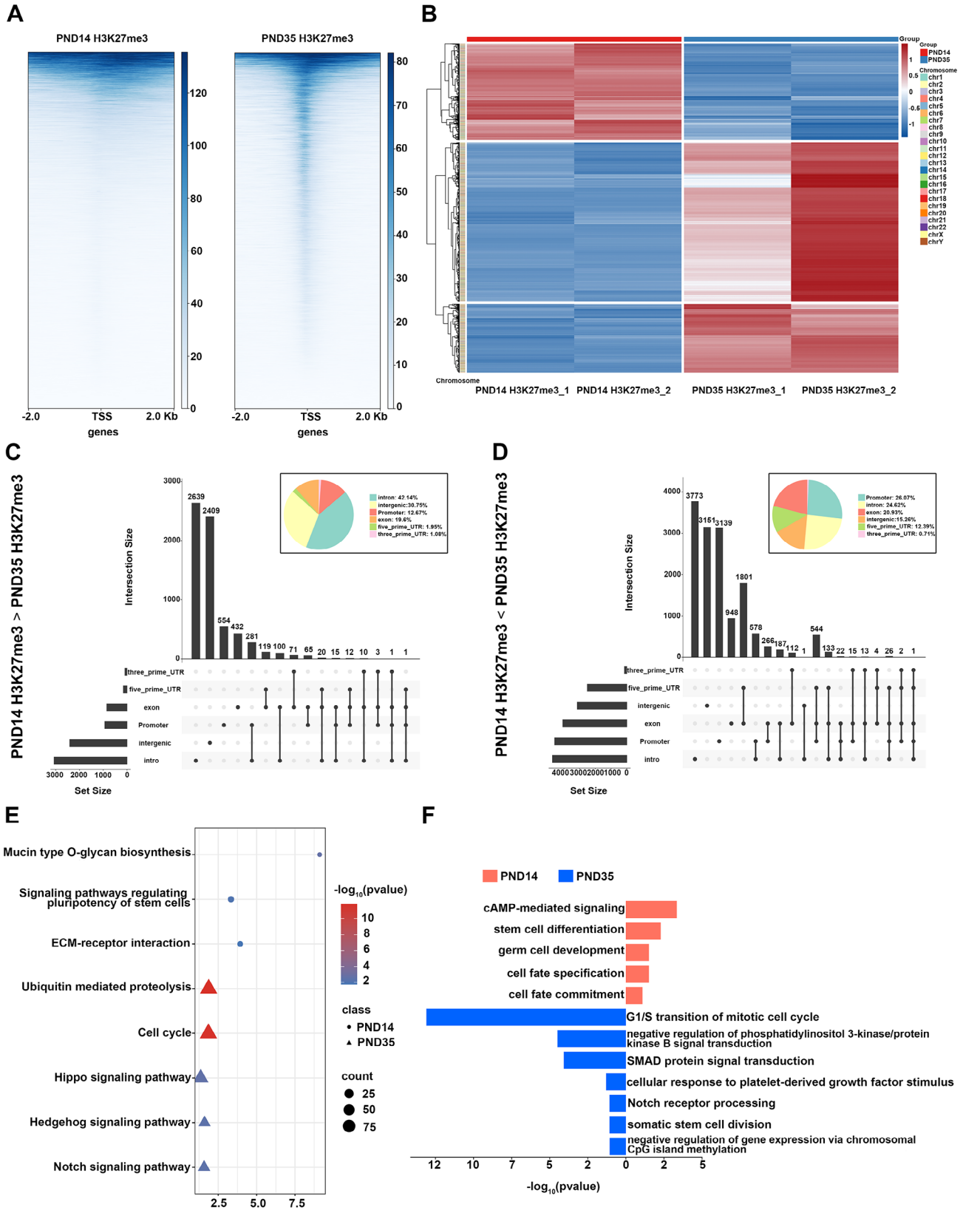

FIGURE 3 | H3K27me3 enrichment profiles in the progenitor Leydig cells and immature Leydig cells. (A) Heatmap of H3K27me3 enrichment at transcription start sites of annotated genes. (B) Differentially enriched H3K27me3 peaks between PND14 and PND35 Leydig cells. (C, D) Upset plots depicting unique sets of H3K27me3-enriched genomic regions in PND14 and PND35 Leydig cells. (E) KEGG pathway enrichment analysis of genes associated with H3K27me3 peaks in PND14 and PND35 Leydig cells. (F) GO biological process enrichment analysis of genes associated with H3K27me3 peaks in PND14 and PND35 Leydig cells.

20472927, 0, Downloaded from https://onlinelibrary.wiley.com/doi/10.1111/andr.70165 by Sun jiandong - Fujian Medical University , Wiley Online Library on [22/12/2025]. See the Terms and Conditions (https://onlinelibrary.wiley.com/terms-and-conditions) on Wiley Online Library for rules of use; OA articles are governed by the applicable Creative Commons License

with developmental signaling pathways, including cell cycle and Notch and Hedgehog signaling pathways (Figure 3E). GO analysis further revealed their involvement in somatic stem cell division and Smad protein signal transduction (Figure 3F). These results indicate an orchestrated epigenetic shift from a pluripotency-permissive chromatin state toward a differentiation-restricted configuration during progenitor cell differentiation.

Surprisingly, steroidogenic genes (*Star*, *Hsd3b1*, *Cyp17a1*, *Hsd17b3*) remained unmarked by H3K27me3 throughout the differentiation process, suggesting these loci are actively protected from polycomb-mediated repression to maintain steroidogenic potential (Figure S6).

3.4 | H3K4me3/H3K27me3-Bivalent Chromatin Domains in Progenitor Leydig Cell Fate Determination

The bivalent chromatin domains marked by both H3K4me3 and H3K27me3, a hallmark of embryonic stem cells, are known to regulate key developmental genes by maintaining them in a poised state for either activation or repression. Our analysis revealed that bivalent promoters account for 24.5% of all promoters in progenitor Leydig cells (Figure 4A), a proportion comparable to that reported in testicular tissue by Cui et al. [16], but notably higher than in embryonic stem cells [17]. Strikingly, we observed a marked predominance of H3K4me3 monovalent-marked genes ($n = 8583$) and bivalent-marked genes ($n = 7269$) over those with H3K27me3-only marks ($n = 1189$).

Notably, critical steroidogenic genes (*Star*, *Hsd3b1*, *Cyp17a1*, *Hsd17b3*) exhibited exclusive H3K4me3 modification, completely lacking the repressive H3K27me3 mark (Figure 4B). Intriguingly, genes with bivalent promoters were predominantly associated with progenitor cell identity markers (e.g., *Arx*, *Pdgfra*, *Nr2f2*, *Ccna2*) and Hedgehog signaling effectors that coordinate Leydig cell differentiation (e.g., *Gli1/2*, *Smo*, *Ptch1/2*).

KEGG pathway analysis revealed a significant enrichment of bivalent genes in "signaling pathways regulating stem cell pluripotency" and "Hedgehog signaling pathway" (Figure 4C,D). Complementary GO analysis further demonstrated their association with biological processes including "sex differentiation", "stem cell population maintenance", "male gonad development", and "spermatogenesis" (Figure 4E).

3.5 | H3K4me3 and H3K27me3 in Adult Leydig Cells Development

Results of immunohistochemistry indicated that H3K4me3 levels increased progressively from immature Leydig cells (PND 28) to mature adult Leydig cells (PND 56), whereas H3K27me3 levels peaked at PND 42 and then slightly declined by PND 56 (Figure S7). The transition from progenitor cells to immature Leydig cells and subsequently to mature adult Leydig cells is accompanied by substantial alterations in H3K4me3 and H3K27me3 modifications at target genes. These epigenetic dynamics may further critically influence the functional maturation of adult Leydig cells.

To elucidate the epigenetic mechanisms governing Leydig cell development, we performed an integrated analysis of transcriptional profiles and histone modification patterns (H3K4me3/H3K27me3) at two critical developmental timepoints: PND28 and PND56. The coordinated enrichment of H3K4me3 and depletion of H3K27me3 drove the significant upregulation of 133 genes during adult Leydig cell development (Cluster A) (Figure 5A). Functional enrichment analysis demonstrated these genes are involved in essential biological processes, including "male gonad development", "testosterone biosynthesis", and "cholesterol metabolism" (Figure 5B). Notably, this cluster contained established markers of mature Leydig cell identity, such as *Hsd17b3*, *Insl3*, and *Sult1e1* (Figure 5C).

Conversely, we identified 903 genes (Cluster B) that were downregulated during maturation, associated with H3K27me3 enrichment and H3K4me3 depletion (Figure 5D). These genes were enriched in developmental signaling pathways (such as Hedgehog signaling and stem cell pluripotency regulation) (Figure 5E) and cell cycle-related processes (including mitotic cell cycle, spindle organization, and sister chromatid segregation) (Figure 5F), suggesting that the suppression of proliferative capacity accompanies terminal differentiation. Protein–protein interaction network analysis of Cluster B genes revealed a core network of 123 targets (Figure 5G). Topological analysis identified ten hub genes through maximal clique centrality scoring, including cell cycle regulators Mki67, Ccna2, and Cdk1 (Figure 5H). This network architecture highlights the coordinated suppression of proliferative programs during adult Leydig cell maturation.

Additionally, we identified transcription factors (TFs) in Clusters A and B, with 13 TFs upregulated and 69 downregulated during adult Leydig cell development (Figure 6A). Among these, *Egr1*, *Nr1d1*, *Rorc*, and *Prox1* are established regulators of steroid metabolism, while *Sox4*, *Gata6*, *Pgr*, *Hmg2*, *Tcf21*, *Six4*, *Ybx3*, *Smad9*, *Runx1*, and *Cebpb* were associated with male reproductive development (Figure 6B). Using the TRRUST dataset, we further constructed a regulatory network of the TFs (Figure 6C), and the fold changes of target genes regulated by TFs are shown in Figure 6D. Target genes were grouped into four clusters based on functional similarity (Figure 6E). Notably, Cluster 1 (*Fgfr4*, *Pdgfra*, *Flt4*, *Csf1r*, *Erbb2*, *Ntrk1*, *Met*, *Insr*), which is enriched for receptor tyrosine kinases, supports cell stemness maintenance, whereas Cluster 2 (*Ccna2*, *Ccne2*, *Ccnd1*, *Ccnd2*), comprising cyclins, is linked to cell proliferation (Figure 6F; Figure S8). The reduced expression of genes in both clusters was found to impair the self-renewal capacity of adult Leydig cells. This TF-target regulatory network expands the molecular framework by which H3K4me3 and H3K27me3 regulate adult Leydig cell development.

4 | Discussion

Histone methylation is an epigenetic mechanism that regulates chromatin structure and gene transcription. Although the dynamic changes in H3K4 and H3K27 methylation during spermatogenesis have been well characterized [18–20], their involvement in the differentiation of testicular somatic cells remains largely underexplored. In this study, we observed that H3K4me3 levels decreased from early progenitor Leydig cells (PND14) to late progenitor Leydig cells (PND21), followed by an increase during

20472927, 0, Downloaded from https://onlinelibrary.wiley.com/doi/10.1111/andr.70165 by Sun jiandong - Fujian Medical University , Wiley Online Library on [22/12/2025]. See the Terms and Conditions (https://onlinelibrary.wiley.com/terms-and-conditions) on Wiley Online Library for rules of use; OA articles are governed by the applicable Creative Commons License

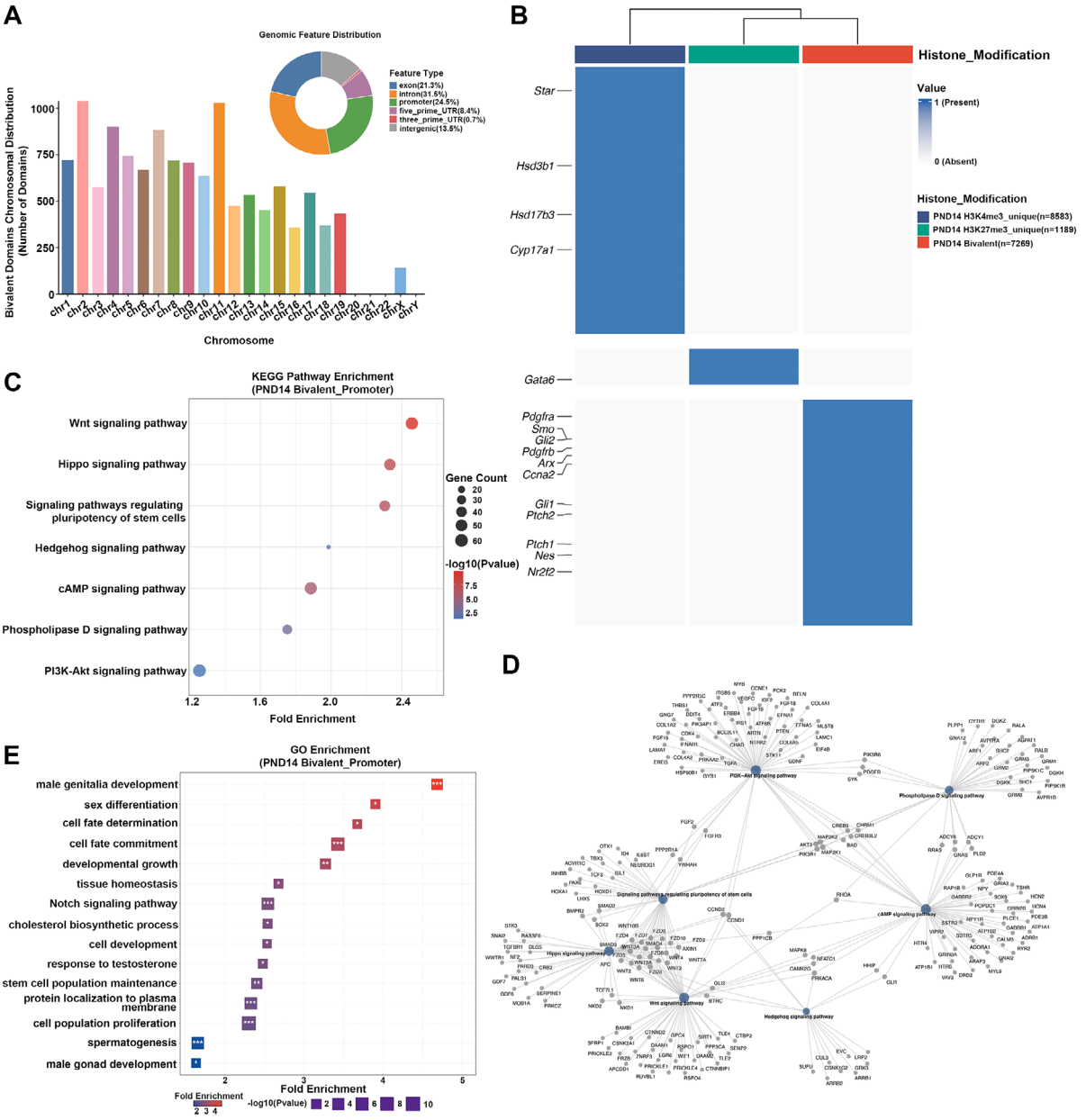

FIGURE 4 | H3K4me3/H3K27me3-bivalent chromatin domains in progenitor Leydig cell fate determination. (A) Genomic distribution of bivalent domains across chromosomes and functional genomic features. (B) Heatmap showing enrichment profiles of genes marked by unique H3K4me3, unique H3K27me3, or bivalent domains. (C) KEGG pathway enrichment bubble plot for genes possessing bivalent promoters in progenitor Leydig cells. (D) Regulatory network of enriched KEGG pathways for genes with bivalent promoters. (E) GO enrichment analysis of biological processes associated with bivalent promoter-containing genes in progenitor Leydig cells.

the transition to immature Leydig cells. Conversely, H3K27me3 levels exhibited a gradual increase throughout the differentiation process from progenitor to immature Leydig cells.

4.1 | Chromatin Bivalency Confers Transcriptional Plasticity in Progenitor Leydig Cells

In the present study, we identified that 24.5% of promoters exhibited a bivalent chromatin state (characterized by concurrent H3K4me3 and H3K27me3 modifications) in progenitor Leydig cells. The predominant enrichment of H3K4me3 over H3K27me3 at progenitor cell markers (e.g., *Pdgfra*, *Arx*, *Nr2f2*, *Ccna2*) reflects a competitive "winner-takes-all" dynamics characteristic of bivalent chromatin resolution. It has been reported that *Pdgfra* inactivation in testicular somatic cells results in an almost complete absence of adult Leydig cells [21, 22]. Similarly, conditional deletion of *Nr2f2* during the prepubertal period prevented the formation of the adult Leydig cell population [23]. Furthermore, progenitor Leydig cells demonstrate high proliferative capacity, correlating with significantly elevated expression of *Ccna2*—a key somatic cell cycle regulator [24]. Collectively, these results position bivalent chromatin resolution as a critical gatekeeper balancing proliferation and differentiation commitment of progenitor cells during postnatal Leydig cell development.

20472927, 0, Downloaded from https://onlinelibrary.wiley.com/doi/10.1111/andr.70165 by Sun jiandong - Fujian Medical University , Wiley Online Library on [22/12/2025]. See the Terms and Conditions (https://onlinelibrary.wiley.com/terms-and-conditions) on Wiley Online Library for rules of use; OA articles are governed by the applicable Creative Commons License

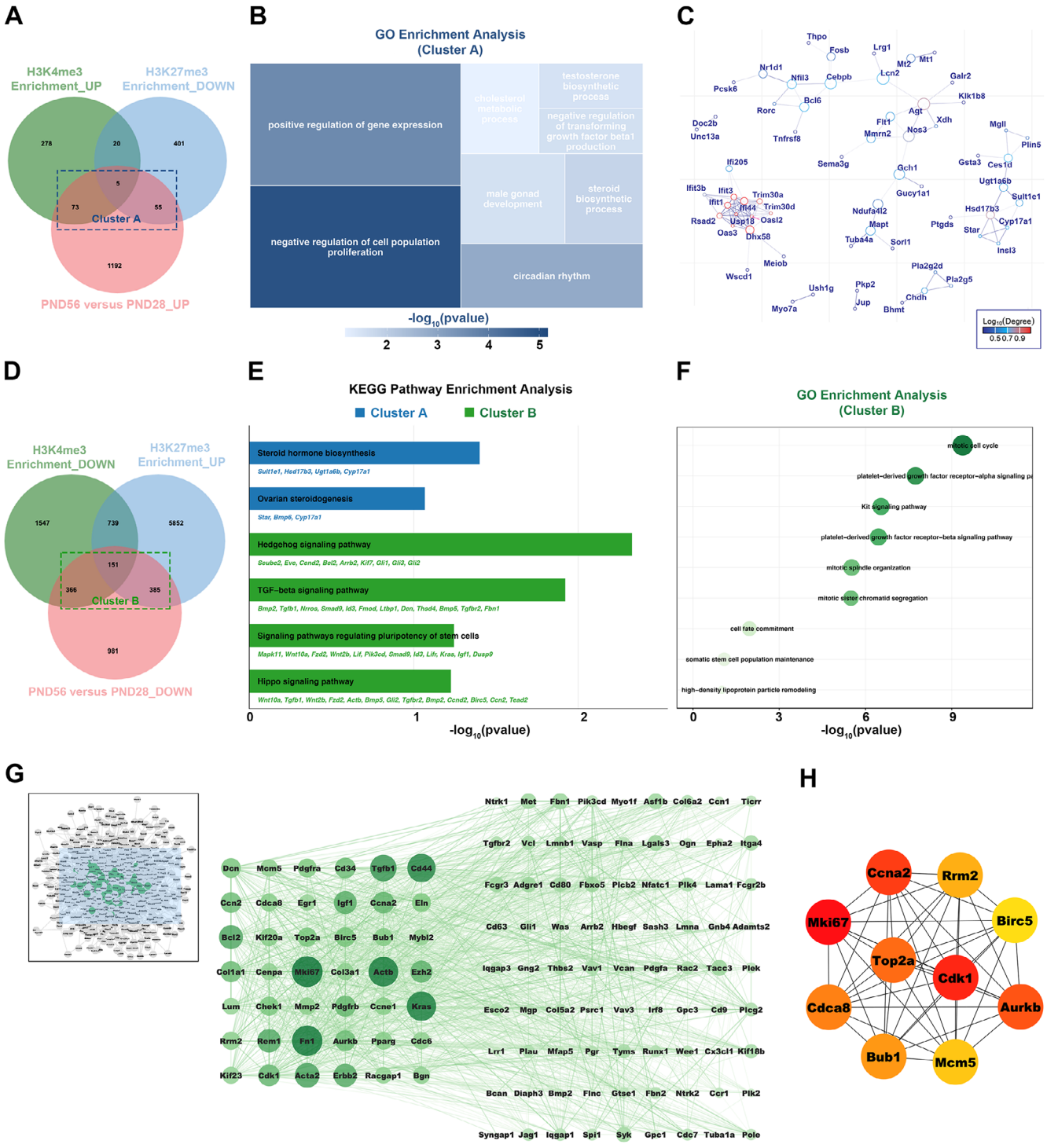

FIGURE 5 | Multi-omics integration identifies epigenetically coordinated gene clusters driving adult Leydig cell differentiation. (A) Venn analysis of transcriptionally upregulated genes exhibiting coordinated epigenetic activation: (i) H3K4me3 peak-gained, (ii) H3K27me3 peak-lost, (iii) RNA-seq upregulated. Cluster A: Epigenetically primed activation. (B) GO enrichment analysis for Cluster A. (C) PPI network of Cluster A. (D) Reciprocal analysis of downregulated genes: (i) H3K4me3 peak-lost, (ii) H3K27me3 peak-gained, (iii) RNA-seq downregulated. Cluster B: Epigenetically silenced. (E) Comparative KEGG pathway analysis of Cluster A vs. B. (F) GO enrichment analysis for Cluster B. (G) Core PPI network of Cluster B. (H) Cluster B hub genes identified via CytoHubba.

20472927, 0, Downloaded from https://onlinelibrary.wiley.com/doi/10.1111/andr.70165 by Sun jiandong - Fujian Medical University , Wiley Online Library on [22/12/2025]. See the Terms and Conditions (https://onlinelibrary.wiley.com/terms-and-conditions) on Wiley Online Library for rules of use; OA articles are governed by the applicable Creative Commons License

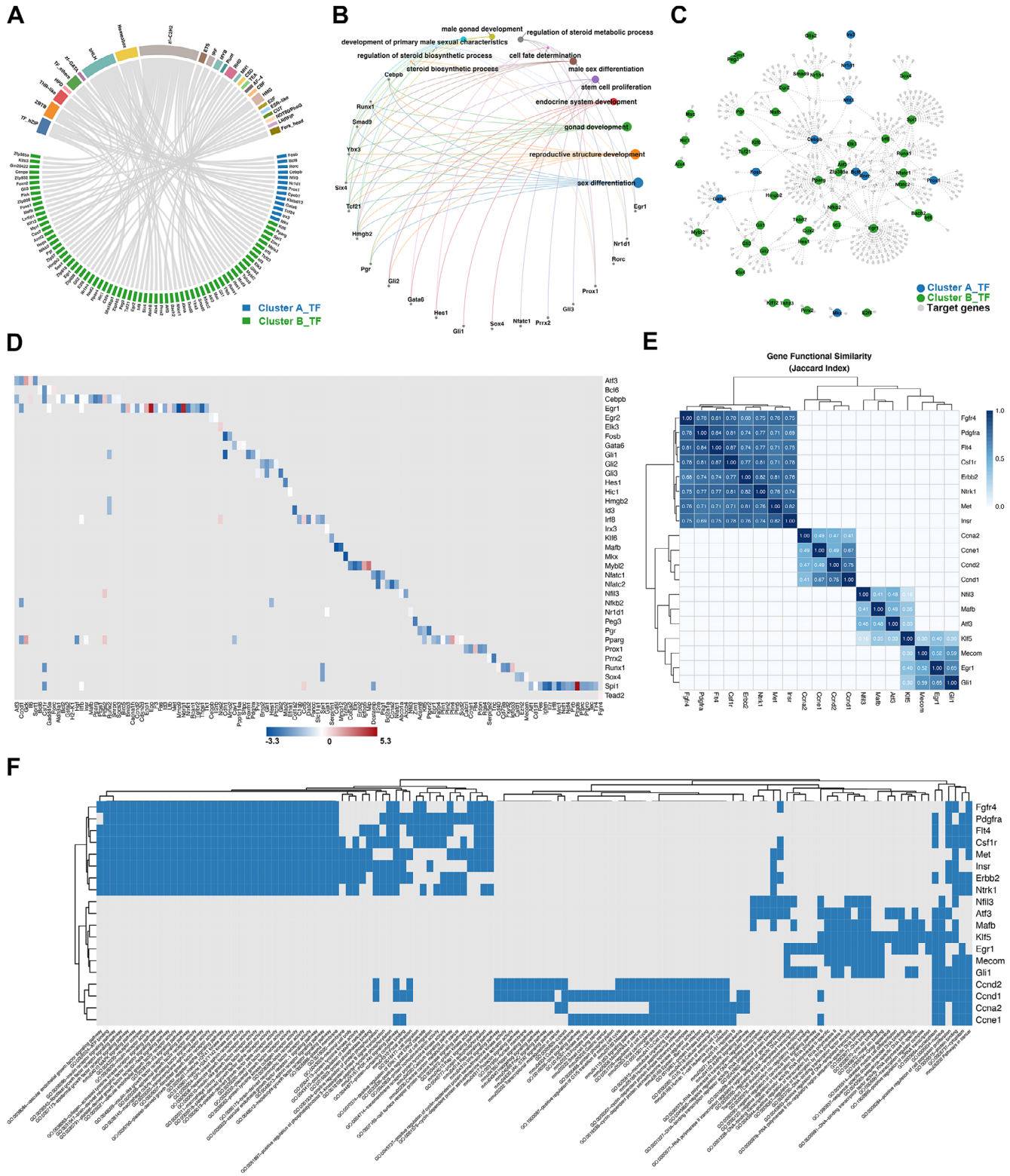

FIGURE 6 | Integrated epigenetic-transcriptional networks coordinate terminal maturation. (A) Transcription factors (TFs) identified within Cluster A (activation-primed) and Cluster B (repression-primed). (B) GO enrichment of biological processes regulated by identified TFs. (C) Experimentally validated TFs-target interactions from the TRRUST database. (D) Transcriptional dynamics (PND56 vs. PND28) of TFs-regulated target genes. (E) Functional enrichment analysis of TFs-targeted genes using DAVID. (F) Comparative functional profiling of target gene networks.

20472927, 0, Downloaded from https://onlinelibrary.wiley.com/doi/10.1111/andr.70165 by Sun jiandong - Fujian Medical University , Wiley Online Library on [22/12/2025]. See the Terms and Conditions (https://onlinelibrary.wiley.com/terms-and-conditions) on Wiley Online Library for rules of use; OA articles are governed by the applicable Creative Commons License

4.2 | Reciprocal Chromatin State Transitions From Progenitor Leydig Cells to Immature Leydig Cells

During the differentiation of progenitor cells into Leydig cells, we observed that several developmental signaling pathways governing this process are precisely coordinated through alternating H3K4me3 activation and H3K27me3 repression: (1) Initially, the Desert hedgehog signaling pathway was activated by H3K4me3 enrichment during early differentiation, but was subsequently silenced through H3K27me3 deposition. (2) Later, H3K27me3 further suppressed both the Notch and Smad signaling pathways to drive Leydig cell formation. This regulatory pattern mirrors that observed in the differentiation cascade of fetal Leydig cells, where the Hedgehog and Notch signaling pathways are sequentially modulated [25].

Interestingly, Leydig cell steroidogenesis was almost exclusively regulated by H3K4me3, with no detectable involvement of H3K27me3. During the lineage transition from progenitor Leydig cells to immature Leydig cells, H3K4me3 enrichment drives enhanced *Cyp11a1* and *Cyp17a*1 transcription activity while initiating *Hsd17b3* expression, thereby establishing testosterone biosynthesis from androstenedione in immature Leydig cells.

4.3 | Integrated Epigenetic-Transcriptional Networks Coordinate Terminal Maturation

Integrated analysis of bulk RNA-seq and CUT&Tag-seq revealed that dynamic remodeling of H3K4me3 and H3K27me3 drives the upregulation of 13 TFs and downregulation of 69 TFs during adult Leydig cell maturation. These TFs are functionally implicated in endocrine system development, male gonad development, cell fate determination, and steroid biosynthesis. Specifically, *Gata6*, *Cebpb*, and *Nr1d1* have been previously reported to promote testosterone production in Leydig cells [26–30]. The simultaneous deletion of *Gata4* and *Gata6* provokes a more severe testicular phenotype than *Gata4* knockout alone, characterized by Leydig cell deficiency and aberrant accumulation of adrenal-like cells in the interstitium [26–28]. *Nr1d1*$^{-/-}$ mice showed diminished fertility in both males and females [31].

Furthermore, the downstream target genes regulated by these transcription factors can be functionally grouped into four categories. *Fgfr4*, *Pdgfra*, *Flt4*, *Csf1r*, *Erbb2*, *Ntrk1*, *Met*, and *Insr* are involved in stem cell factor receptor activity. Notably, the expression levels of *Fgfr4*, *Insr*, and *Flt4* were found to be upregulated. Neirijnck et al. [32] reported that phospholipase C (PLC) accumulation is secondary to *Insr* deletion specifically in differentiated adult Leydig cells. Lin et al. [33] also suggested that the Fgf9-Fgfr4 signaling pathway plays a role in postnatal testicular development and Leydig cell steroidogenesis. Moreover, cyclins such as *Ccne1*, *Ccna2*, *Ccnd1*, and *Ccnd2*, which are transcriptionally regulated by factors including *Nfatc1*, *Prox1*, and *Egr1* (as predicted by the TRRUST database), exhibit decreased expression during adult Leydig cell maturation. This decline ultimately contributes to the loss of proliferative capacity in mature Leydig cells.

5 | Conclusion

In conclusion, our study identifies the H3K4me3/H3K27me3-TFs-target gene axis as a central regulatory mechanism governing postnatal Leydig cell differentiation, thereby elucidating how this pathway facilitates steroidogenic potential while concurrently suppressing stemness characteristics. Nevertheless, the potential synergistic interactions between H3K4me3/H3K27me3 and other epigenetic modifications (e.g., H3K27ac, DNA methylation) in regulating Leydig cell differentiation warrant further investigation.

Author Contributions

Shie Wang: conceptualization, funding acquisition, project administration, supervision, and writing – review & editing. **Jiandong Sun**: conceptualization, project administration, funding acquisition, supervision, visualization, and writing – original draft. **Xiuli Lian**: conceptualization, formal analysis, investigation, methodology, and software. **Shanshan Luo**: data curation, formal analysis, investigation, and methodology. **Zihang Lin**: formal analysis, investigation, and methodology. **Lvjing Luo**: methodology and software. **Mei Zheng**: software and validation. **Dini Zhang**: software and validation. **Zeyu Lin**: formal analysis and validation. **Xuanyi Wang**: software.

Acknowledgments

We thank Ling Lin from the Public Technology Service Center of Fujian Medical University for her technical assistance.

Ethics Statement

This study was approved by the local ethics committee of Fujian Medical University (code of ethics: LLSLBH-20210930–002).

Conflicts of Interest

The authors declare no conflicts of interest.

Data Availability Statement

The data that support the findings of this study are available from the corresponding author upon reasonable request.

Funding

The work was supported by National Natural Science Foundation of China (grant/award number: 82501929), Science and Technology Innovation Foundation of Fujian Province (grant/award number: 2023Y9003, 2024Y9092), Fujian Province financial special plan project (grant/award number: 22SCZZX017), Fujian Medical University high-level talents scientific research start-up funding project (grant/award number: XRCZX2024039).

References

1. B. R. Zirkin and V. Papadopoulos, "Leydig Cells: Formation, Function, and Regulation," *Biology of Reproduction* 99, no. 1 (2018): 101–111, https://doi.org10.1093/biolre/ioy059.

2. L. Ye, X. Li, L. Li, H. Chen, and R. S. Ge, "Insights Into the Development of the Adult Leydig Cell Lineage From Stem Leydig Cells," *Frontiers in Physiology* 8 (2017): 430, https://doi.org10.3389/fphys.2017.00430.

3. B. M. Lawrence, L. O'Donnell, L. B. Smith, and D. Rebourcet, "New Insights Into Testosterone Biosynthesis: Novel Observations From HSD17B3 Deficient Mice," *International Journal of Molecular Sciences* 23, no. 24 (2022), https://doi.org10.3390/ijms232415555.

20472927, 0, Downloaded from https://onlinelibrary.wiley.com/doi/10.1111/andr.70165 by Sun jiandong - Fujian Medical University , Wiley Online Library on [22/12/2025]. See the Terms and Conditions (https://onlinelibrary.wiley.com/terms-and-conditions) on Wiley Online Library for rules of use; OA articles are governed by the applicable Creative Commons License

4. P. Sararols, I. Stevant, Y. Neirijnck, et al., "Specific Transcriptomic Signatures and Dual Regulation of Steroidogenesis between Fetal and Adult Mouse Leydig Cells," *Frontiers in Cell and Developmental Biology* 9 (2021): 695546, https://doi.org10.3389/fcell.2021.695546.

5. M. Varjosalo and J. Taipale, "Hedgehog: Functions and Mechanisms," *Genes & Development* 22, no. 18 (2008): 2454–2472, https://doi.org10.1101/gad.1693608.

6. Y. Kawai, J. Noguchi, K. Akiyama, et al., "A Missense Mutation of the Dhh Gene Is Associated With Male Pseudohermaphroditic Rats Showing Impaired Leydig Cell Development," *Reproduction (Cambridge, England)* 141, no. 2 (2011): 217–225, https://doi.org10.1530/REP-10-0006.

7. X. Li, Z. Wang, Z. Jiang, et al., "Regulation of Seminiferous Tubule-associated Stem Leydig Cells in Adult Rat Testes," *Proceedings of National Academy of Sciences* 113, no. 10 (2016): 2666–2671, https://doi.org10.1073/pnas.1519395113.

8. X. Li, Y. Fang, L. Chen, H. Quan, Y. Wang, and R. S. Ge, "Bone Morphogenetic Protein 4 Inhibits Rat Stem/Progenitor Leydig Cell Development and Regeneration via SMAD-dependent and SMAD-independent Signaling," *Cell Death & Disease* 13, no. 12 (2022): 1039, https://doi.org10.1038/s41419-022-05471-8.

9. Y. Shima, K. Miyabayashi, T. Baba, et al., "Identification of an Enhancer in the Ad4BP/SF-1 Gene Specific for Fetal Leydig Cells," *Endocrinology* 153, no. 1 (2012): 417–425, https://doi.org10.1210/en.2011-1407.

10. T. Karpova, K. Ravichandiran, L. Insisienmay, D. Rice, V. Agbor, and L. L. Heckert, "Steroidogenic Factor 1 Differentially Regulates Fetal and Adult Leydig Cell Development in Male Mice," *Biology of Reproduction* 93, no. 4 (2015): 83, https://doi.org10.1095/biolreprod.115.131193.

11. Y. Yang, Z. Li, X. Wu, et al., "Direct Reprogramming of Mouse Fibroblasts Toward Leydig-Like Cells by Defined Factors," *Stem Cell Reports* 8, no. 1 (2017): 39–53, https://doi.org10.1016/j.stemcr.2016.11.010.

12. C. Dulac, "Brain Function and Chromatin Plasticity," *Nature* 465, no. 7299 (2010): 728–735, https://doi.org10.1038/nature09231.

13. R. Margueron and D. Reinberg, "The Polycomb Complex PRC2 and Its Mark in Life," *Nature* 469, no. 7330 (2011): 343–349, https://doi.org10.1038/nature09784.

14. H. Santos-Rosa, R. Schneider, A. J. Bannister, et al., "Active Genes Are Tri-Methylated at K4 of Histone H3," *Nature* 419, no. 6905 (2002): 407–411, https://doi.org10.1038/nature01080.

15. K. Hyun, J. Jeon, K. Park, and J. Kim, "Writing, Erasing and Reading Histone Lysine Methylations," *Experimental & Molecular Medicine* 49, no. 4 (2017): e324, https://doi.org10.1038/emm.2017.11.

16. P. Cui, W. Liu, Y. Zhao, et al., "Comparative Analyses of H3K4 and H3K27 Trimethylations Between the Mouse Cerebrum and Testis," *Genomics, Proteomics & Bioinformatics* 10, no. 2 (2012): 82–93, https://doi.org10.1016/j.gpb.2012.05.007.

17. T. S. Mikkelsen, M. Ku, D. B. Jaffe, et al., "Genome-wide Maps of Chromatin State in Pluripotent and Lineage-Committed Cells," *Nature* 448, no. 7153 (2007): 553–560, https://doi.org10.1038/nature06008.

18. L. Xu, W. Xu, D. Li, et al., "FANCI Plays an Essential Role in Spermatogenesis and Regulates Meiotic Histone Methylation," *Cell Death & Disease* 12, no. 8 (2021): 780, https://doi.org10.1038/s41419-021-04034-7.

19. J. An, J. Qin, Y. Wan, et al., "Histone Lysine Methylation Exhibits a Distinct Distribution During Spermatogenesis in Pigs," *Theriogenology* 84, no. 9 (2015): 1455–1462, https://doi.org10.1016/j.theriogenology.2015.07.013.

20. Y. Cai, M. Deng, Z. Liu, et al., "EZH2 expression and Its Role in Spermatogonial Stem Cell Self-Renewal in Goats," *Theriogenology* 155 (2020): 222–231, https://doi.org10.1016/j.theriogenology.2020.06.013.

21. J. Schmahl, K. Rizzolo, and P. Soriano, "The PDGF Signaling Pathway Controls Multiple Steroid-Producing Lineages," *Genes & Development* 22, no. 23 (2008): 3255–3267, https://doi.org10.1101/gad.1723908.

22. J. Brennan, C. Tilmann, and B. Capel, "Pdgfr-alpha Mediates Testis Cord Organization and Fetal Leydig Cell Development in the XY Gonad," *Genes & Development* 17, no. 6 (2003): 800–810, https://doi.org10.1101/gad.1052503.

23. J. Qin, M. J. Tsai, and S. Y. Tsai, "Essential Roles of COUP-TFII in Leydig Cell Differentiation and Male Fertility," *PLoS ONE* 3, no. 9 (2008): e3285, https://doi.org10.1371/journal.pone.0003285.

24. R. S. Ge and M. P. Hardy, "Decreased Cyclin A2 and Increased Cyclin G1 Levels Coincide With Loss of Proliferative Capacity in Rat Leydig Cells During Pubertal Development," *Endocrinology* 138, no. 9 (1997): 3719–3726, https://doi.org10.1210/endo.138.9.5387.

25. K. Jiang and J. S. Jorgensen, "Fetal Leydig Cells: What We Know and What We Don," *Molecular Reproduction and Development* 91, no. 3 (2024): e23739, https://doi.org10.1002/mrd.23739.

26. M. B. Padua, T. Jiang, D. A. Morse, S. C. Fox, H. M. Hatch, and S. G. Tevosian, "Combined Loss of the GATA4 and GATA6 Transcription Factors in Male Mice Disrupts Testicular Development and Confers Adrenal-Like Function in the Testes," *Endocrinology* 156, no. 5 (2015): 1873–1886, https://doi.org10.1210/en.2014-1907.

27. N. L. Manuylov, B. Zhou, Q. Ma, S. C. Fox, W. T. Pu, and S. G. Tevosian, "Conditional Ablation of Gata4 and Fog2 Genes in Mice Reveals Their Distinct Roles in Mammalian Sexual Differentiation," *Developmental Biology* 353, no. 2 (2011): 229–241, https://doi.org10.1016/j.ydbio.2011.02.032.

28. G. M. Penny, R. B. Cochran, M. Pihlajoki, et al., "Probing GATA Factor Function in Mouse Leydig Cells via Testicular Injection of Adenoviral Vectors," *Reproduction (Cambridge, England)* 154, no. 4 (2017): 455–467, https://doi.org10.1530/REP-17-0311.

29. C. Li, L. Zhang, T. Ma, et al., "Bisphenol A Attenuates Testosterone Production in Leydig Cells via the Inhibition of NR1D1 Signaling," *Chemosphere* 263 (2021): 128020, https://doi.org10.1016/j.chemosphere.2020.128020.

30. D. Xing, Y. Jin, and D. Sun, "Protective Effect of TNFAIP3 on Testosterone Production in Leydig Cells Under an Aging Inflammatory Microenvironment," *Archives of Gerontology and Geriatrics* 117 (2024): 105274, https://doi.org10.1016/j.archger.2023.105274.

31. H. Cho, X. Zhao, M. Hatori, et al., "Regulation of Circadian Behaviour and Metabolism by REV-ERB-Alpha and REV-ERB-beta," *Nature* 485, no. 7396 (2012): 123–127, https://doi.org10.1038/nature11048.

32. Y. Neirijnck, P. Calvel, K. R. Kilcoyne, et al., "Insulin and IGF1 Receptors Are Essential for the Development and Steroidogenic Function of Adult Leydig Cells," *Faseb Journal* 32, no. 6 (2018): 3321–3335, https://doi.org10.1096/fj.201700769RR.

33. Y. M. Lin, C. C. Tsai, C. L. Chung, et al., "Fibroblast Growth Factor 9 Stimulates Steroidogenesis in Postnatal Leydig Cells," *International Journal of Andrology* 33, no. 3 (2010): 545–553, https://doi.org10.1111/j.1365-2605.2009.00966.x.

Supporting Information

Additional supporting information can be found online in the Supporting Information section.

Figure S1: Expression levels of H3K4me3/H3K27me3-modifying enzymes (writers/erasers) visualized by organ chart across Leydig cell developmental stages. SPG, spermatogonia; SPC, spermatocytes; SPT, spermatids/sperms; SC: Sertoli cells; LC, Leydig cells; PTM: peritubular myoid cells; EC: endothelial cells; SMC: vascular smooth muscle cells; Immune: immune cell. **Figure S2**: Identification of Leydig cell subpopulations. (A) Representative immunofluorescence images showing NR2F2 expression in progenitor Leydig cells. Scale bar, 100 μm. (B) HSD3B1 staining in immature Leydig cells and adult Leydig cells. Scale bar, 50 μm. (C) Representative immunofluorescence images showing HSD17B3 expression in adult Leydig cells. Scale bar, 50 μm. **Figure S3**: Representative immunofluorescence images showing the expression of H3K4me3/H3K27me3-modifying enzymes (writers/erasers)

20472927, 0, Downloaded from https://onlinelibrary.wiley.com/doi/10.1111/andr.70165 by Sun jiandong - Fujian Medical University , Wiley Online Library on [22/12/2025]. See the Terms and Conditions (https://onlinelibrary.wiley.com/terms-and-conditions) on Wiley Online Library for rules of use; OA articles are governed by the applicable Creative Commons License

in developing Leydig cells. Developmental stages are indicated as: PND14 and PND21, progenitor Leydig cells; PND28 and PND35, immature Leydig cells. Scale bar, 50 μm. **Figure S4**: The expression of target genes following H3K4me3 writers/erasers knockdown. (A) Transcript abundance (RNA-seq read counts) of major H3K4me3 methyltransferases (writers) and demethylases (erasers) in PND28 immature Leydig cells. (B) The mRNA expression of *Star*, *Cyp17a1*, and *Hsd17b3* upon *Kmt2c* knockdown in immature Leydig cells. (C) The mRNA expression of *Star*, *Cyp17a1*, and *Hsd17b3* upon *Kdm5c* knockdown in immature Leydig cells. Student's *t*-test. Significance levels: $*p < 0.05$, $**p < 0.01$, $***p < 0.001$. Bars indicate SD. **Figure S5**: IGV genome browser views of representative H3K4me3 peaks in progenitor (PND14) and immature (PND35) Leydig cells. **Figure S6**: IGV genome browser views of representative H3K27me3 peaks in progenitor (PND14) and immature (PND35) Leydig cells. **Figure S7**: Representative immunohistochemical staining for H3K4me3 and H3K27me3 in immature (PND28, 35) and adult (PND56) Leydig cells. Scale bar, 50 μm. **Figure S8**: Analysis of gene expression by RT-qPCR in Leydig cells at PND28 and PND56. Student's *t*-test. Significance levels: $*p < 0.05$, $**p < 0.01$, $***p < 0.001$. Bars indicate SD. RNA sequencing **Table S1**: Antibody Information **Table S2:** Sequence information of primers for RT-PCR

20472927, 0, Downloaded from https://onlinelibrary.wiley.com/doi/10.1111/andr.70165 by Sun jiandong - Fujian Medical University , Wiley Online Library on [22/12/2025]. See the Terms and Conditions (https://onlinelibrary.wiley.com/terms-and-conditions) on Wiley Online Library for rules of use; OA articles are governed by the applicable Creative Commons License